Electronic Supplementary Material (ESI) for Journal of Materials Chemistry A.
This journal is © The Royal Society of Chemistry 2017

Pillar[n]arene based porous polymers for rapid pollutant removal from water

Shang Lan, Shuaijun Zhan, Jiaming Ding, Jiaqi Ma and Da Ma

Department of Chemistry, Fudan University

Table of Contents

General experimental S2
Syntheses of P-PAP[n]s S3
Methods for pollutant adsorption experiments S4
FT-IR spectra of P-PAP[6] and monomers S6
Solid-state NMR of P-PAP[6] and DEPA[6] S7
BET analysis of P-PAP[6] S8
SEM images of P-PAP[6] S9
Standard curve of paraquat S10
Flow-through adsorption experiments of different pollutants S11
Paraquat adsorption kinetics of P-PAP[5] and AC S12
Regeneration experiments S13
^{1}H NMR demonstration of host-guest interaction S14
Paraquat removal performance of various adsorbents S15
References S17

General experimental

All reagents and solvents were purchased from commercial suppliers and used without further purification. DMPA[5] and DEPA[6] were prepared according to literature procedures.[1,2] Aqueous solutions of pollutants were prepared using deionized water at neutral pH.

Ultraviolet-visible (UV-Vis) spectroscopy was performed on a Cary 100 Agilent UV-Vis spectrometer. The morphology was imaged by scanning electron microscopy (SEM, Phenom Prox, operated at 15 kV). Fourier transform infrared spectroscopy (FT-IR) spectra were recorded on a Thermo Nicolet iS10 spectrometer. Solid-state NMR spectra were recorded on a BRUKER 400WB AVANCE III. The surface area and pore size distribution analysis of polymers was performed on a Quantachrome Autosorb-iQ gas adsorption and pore size analyzer, using N_2 adsorption and desorption at 77 K. Samples were degassed at 80 °C under high vacuum for 24 h prior to the N_2 adsorption and desorption analysis.

Syntheses of P-PAP[n]s

P-PAP[5]: A solution of dimethylpillar[5]arene (DMPA[5], 2.25 g, 3.0 mmol) and BBr_3 (5.5 mL, 60 mmol) in dichloromethane (100 mL) was stirred at r.t. for 24 h. The reaction was quenched with water (200 mL). The precipitate was filtered and washed with water to yield PA[5] (1.53 g, 2.5 mmol) as a white solid. A suspension of PA[5] (1.53 g, 2.5 mmol), tetrafluoroterephthalonitrile (1.50 g, 7.5 mmol) and K_2CO_3 (4.2 g, 30 mmol) in DMF (100 mL) was heated at 90 °C for 48 h under N_2. The precipitate was filtered and washed with 10% HCl (100 mL), H_2O (300 mL), methanol (100 mL) and CH_2Cl_2 (100 mL). The solid was dried under high vacuum to yield P-PAP[5] as a yellow solid (1.3 g, 48%).

P-PAP[6]: A solution of diethylpillar[6]arene (DEPA[6], 0.48 g, 0.45 mmol) and BBr_3 (1.5 mL, 16 mmol) in dichloromethane (30 mL) was stirred at r.t. for 24 h. The reaction was quenched with water (100 mL). The precipitate was filtered and washed with water to yield PA[6] (0.29 g, 0.40 mmol) as a white solid. A suspension of PA[6] (0.29 g, 0.40 mmol), tetrafluoroterephthalonitrile (0.24 g, 1.2 mmol) and K_2CO_3 (1.0 g, 7.2 mmol) in DMF (20 mL) was heated at 90 °C for 48 h under N_2. The precipitate was filtered and washed with 5% HCl (50 mL), H_2O (200 mL), methanol (50 mL) and CH_2Cl_2 (50 mL). The solid was dried under high vacuum to yield P-PAP[6] as a yellow solid (0.10 g, 20%).

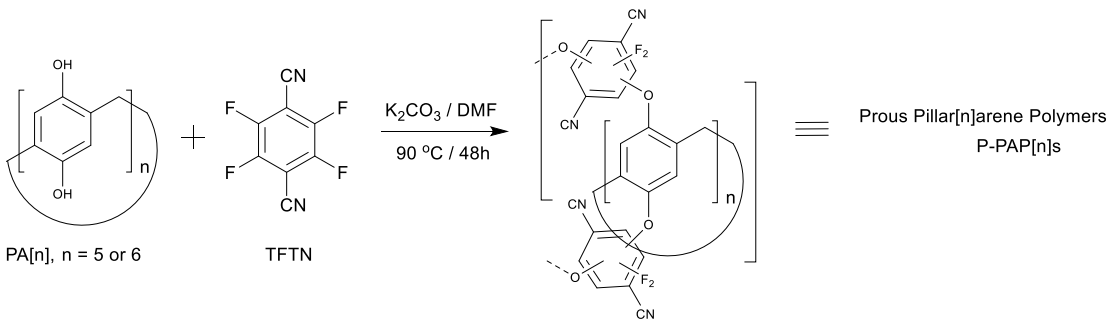

Scheme S1. Syntheses of P-PAP[n]s (n = 5 or 6).

Methods for pollutant adsorption experiments

Pollutant adsorption experiments were carried out at room temperature. The pollutant concentration was determined with UV-Vis spectroscopy according to a standard curve. The Cu^{2+} concentration was determined by adding a solution of DDTC (Sodium diethyldithiocarbamate, 1 mM, 1 mL) into a Cu^{2+} solution (2 mL), and subsequently recording the UV-Vis absorbance.[3]

The pollutant removal efficiency was calculated with the following equation:

$$Pollutant\ removal\ efficiency = \frac{(C_0 - C_t)}{C_0} \times 100\%$$

C_0 (mmol l^{-1}) and C_t (mmol l^{-1}) are the concentrations of pollutant either before or after adsorption.

The amount of adsorbed pollutant was determined by the following equation:

$$q_t = \frac{(C_0 - C_t)VM_w}{m}$$

q_t (mg g^{-1}) is the amount of pollutant adsorbed per gram of adsorbent at time t (min); V (L) is the volume of the solution; M_w is the molar mass of the pollutant; m (g) is the mass of the adsorbent.

Flow-through adsorption experiments: The adsorbent (3 mg) was washed with H_2O (3 mL) for 5min. The suspension was loaded into a syringe and passed through a 0.2 μm membrane filter to form a thin layer of adsorbent. A solution of paraquat (0.1 mM, 3 mL) was passed through the adsorbent layer. The concentration of paraquat in the filtrate was determined with UV-Vis spectroscopy (257 nm).

Adsorption kinetics: The polymer (20 mg) was washed with H_2O (20 mL) for 5min and then filtered. The polymer was added into a solution of paraquat (0.1 mM, 20 ml) and stirred at r.t.. Samples were taken at certain time points and the suspension was filtered. The concentration of paraquat in the filtrate was determined with UV-Vis spectroscopy (257 nm).

The pseudo-second-order kinetic model was used to fit the experimental data:

$$\frac{t}{q_t} = \frac{t}{q_e} + \frac{1}{k_2 q_e^2}$$

Where q_t and q_e are the amount of pollutant adsorbed per g of adsorbent at time t (min)

and equilibrium, and k_2 is the rate constant.

Adsorption capacity: The polymer (5 mg) was washed with H_2O (5 mL) for 5 min and then filtered. The polymer was added into a solution of paraquat (5 mL) with an initial concentration of 0.6 mM, 0.7 mM, 0.8 mM, 0.9 mM, 1.0 mM, 1.6 mM, and 2.0 mM. The suspension was stirred for 10 min and then filtered. The concentration of paraquat in the filtrate was determined with UV-Vis spectroscopy (257 nm).

The adsorption data were fitted with Langmuir isotherm model by the following equation:

$$q_e = \frac{q_{max} b C_e}{1 + b C_e}$$

Where q_e (mg g^{-1}) is the amount of pollutant adsorbed at equilibrium, C_e (mM) is the residual pollutant concentration at equilibrium, q_{max} (mg g^{-1}) is the maximum adsorption capacity of pollutants, and b is the equilibrium constant.

Guest displacement assays: The polymer (3 mg) was washed with H_2O (3 mL) for 5 min and then filtered. The polymer was added to a solution of paraquat (0.1 mM, 3 mL) and stirred for 10 min. The suspension was filtered and the concentration of paraquat in the filtrate was determined by UV-Vis spectroscopy (257 nm). The paraquat loaded polymer was added into either a solution of hexanediamine dichlorohydride salt (4 mM, 3 mL) or $CaCl_2$ (4 mM, 3 mL), and stirred for 5 min. The suspension was filtered and the concentration of paraquat in the filtrate was determined with UV-Vis spectroscopy (257 nm).

Regeneration experiments: the polymer (3 mg) was washed with H_2O (3 mL) for 5 min and then filtered. The polymer was added into a solution of paraquat (0.1 mM, 3 mL) and stirred for 10 min. The suspension was filtered and the concentration of paraquat in the filtrate was determined with UV-Vis spectroscopy. The polymer was regenerated by washing with MeOH (3 mL) for 5 min and filtration. The adsorption/desorption was repeated for five cycles.

FT-IR spectra of P-PAP[6] and monomers

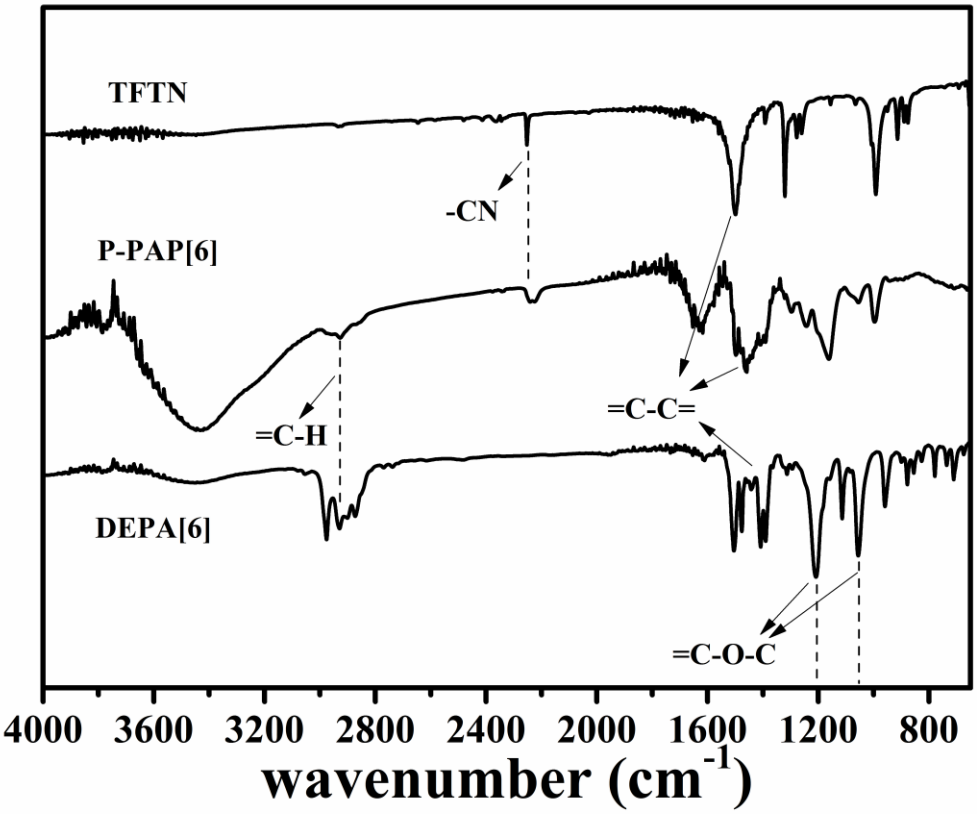

Fig. S1 FT-IR spectra of TFTN, P-PAP[6] and DEPA[6].

Solid-state NMR of P-PAP[6] and DEPA[6]

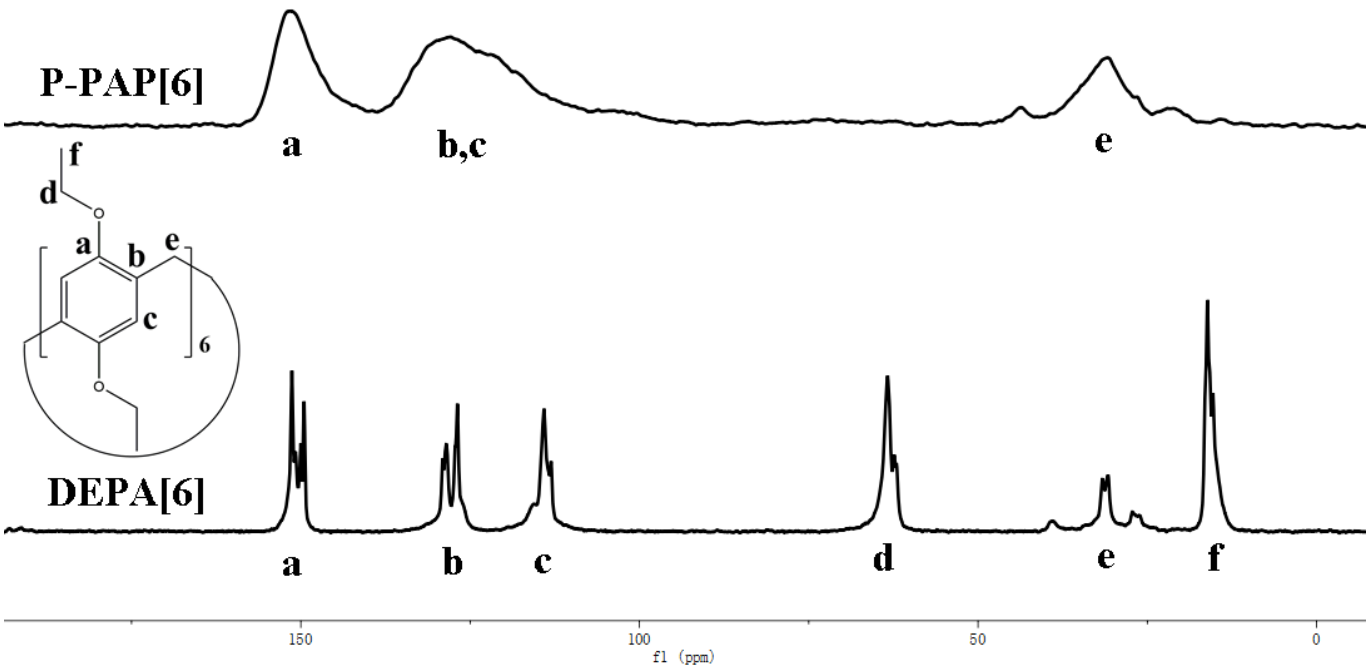

Fig. S2 Solid-state NMR of DEPA[6] and P-PAP[6].

BET analysis of P-PAP[6]

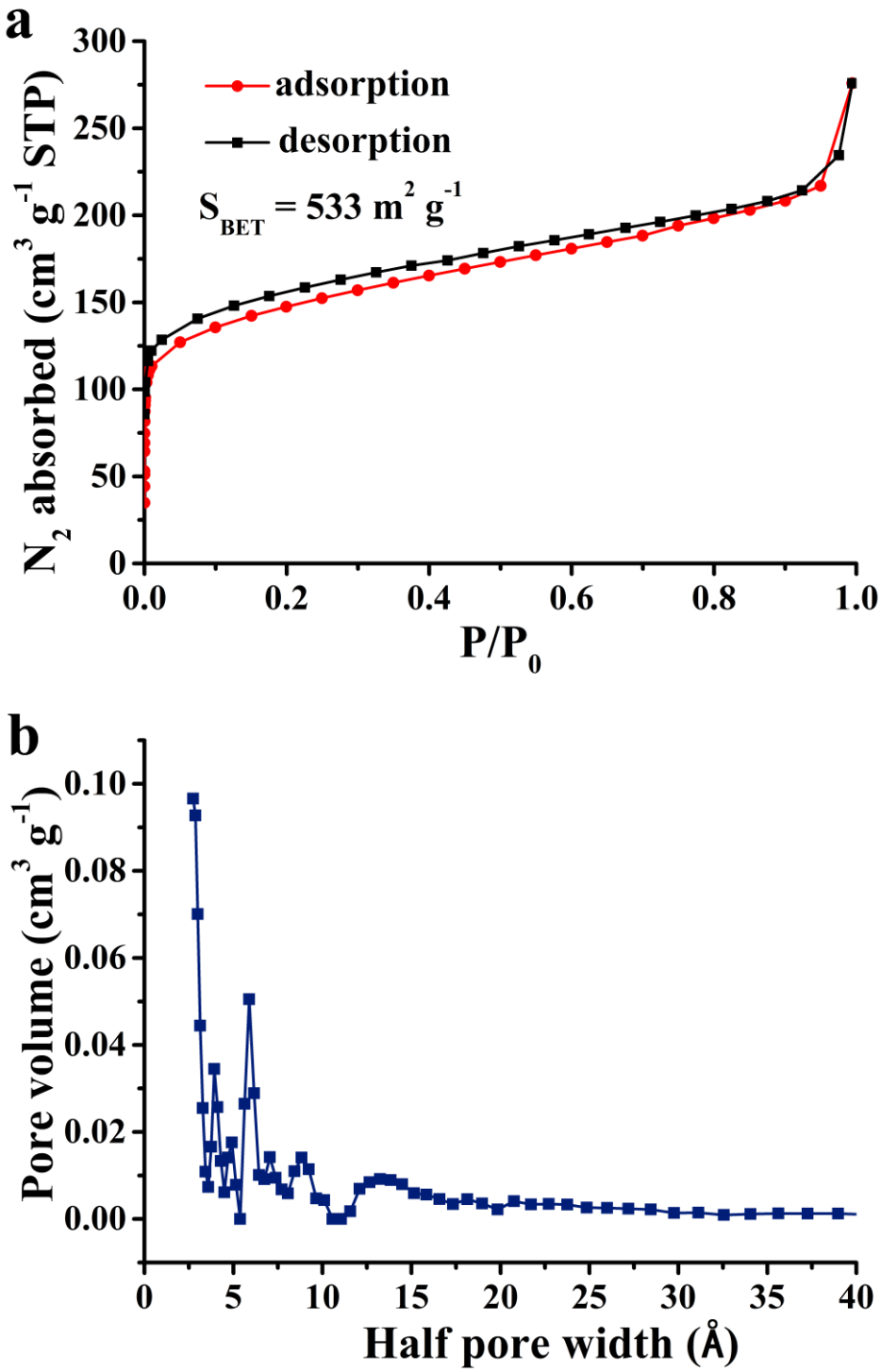

Fig. S3 (a) N_2 sorption and desorption isotherms of P-PAP[6]. (b) The cumulative pore volume (half pore width) of P-PAP[6] obtained by NLDFT analysis.

SEM images of P-PAP[6]

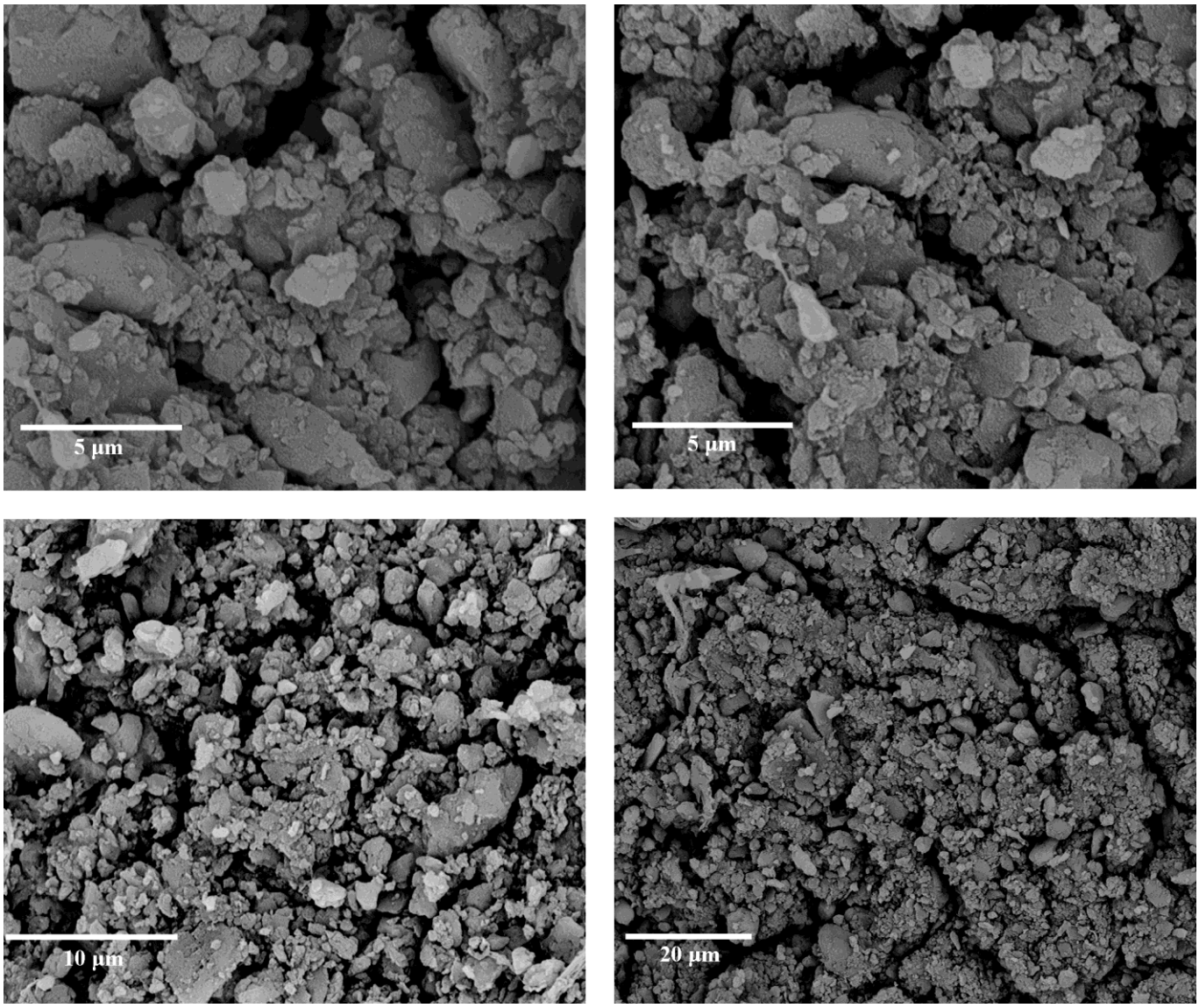

Fig. S4 SEM images of P-PAP[6]

Standard curve of paraquat

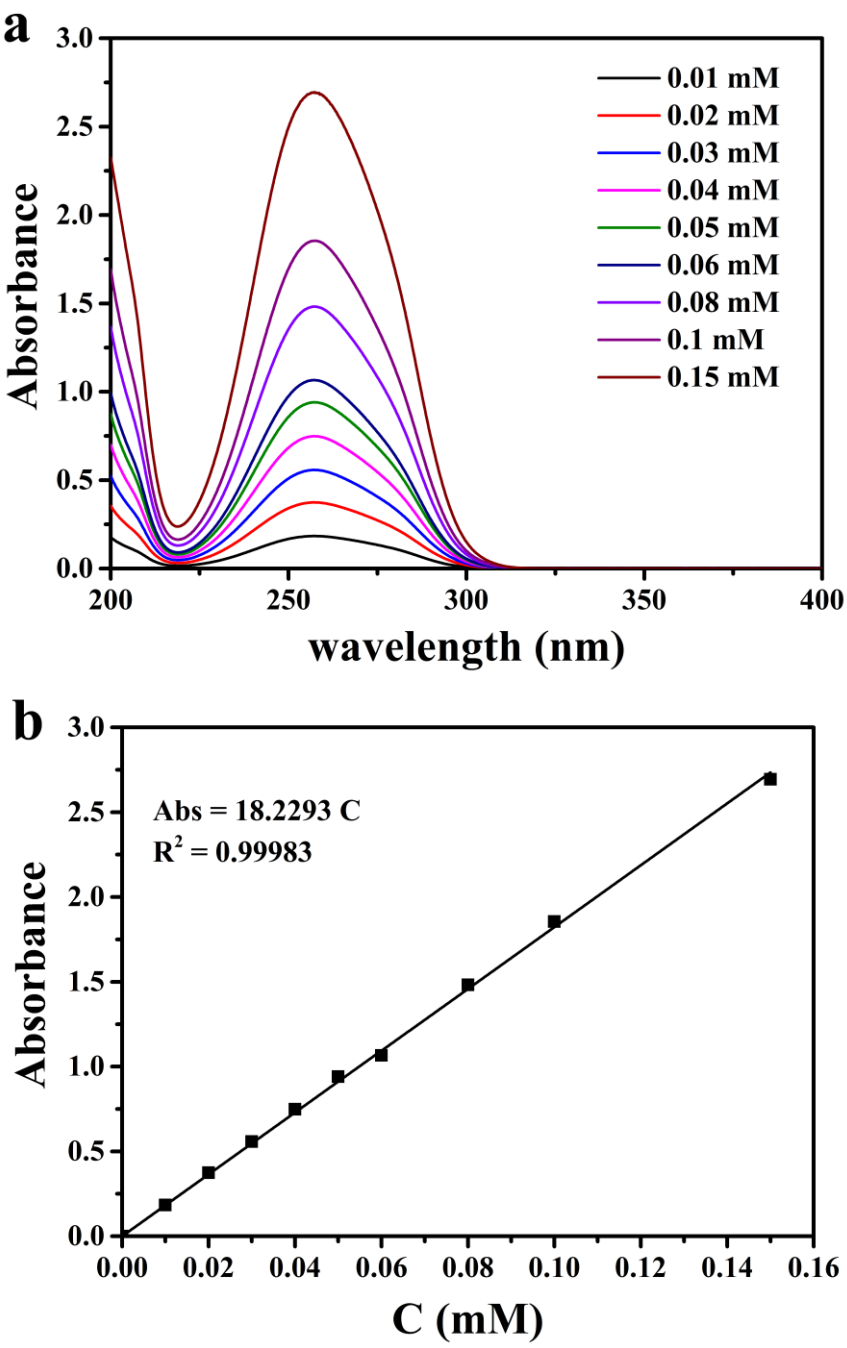

Fig. S5 a) UV-Vis spectra of paraquat of different concentrations. b) Standard curve plotted based on the absorbance at 257 nm.

Flow-through adsorption experiments of different pollutants

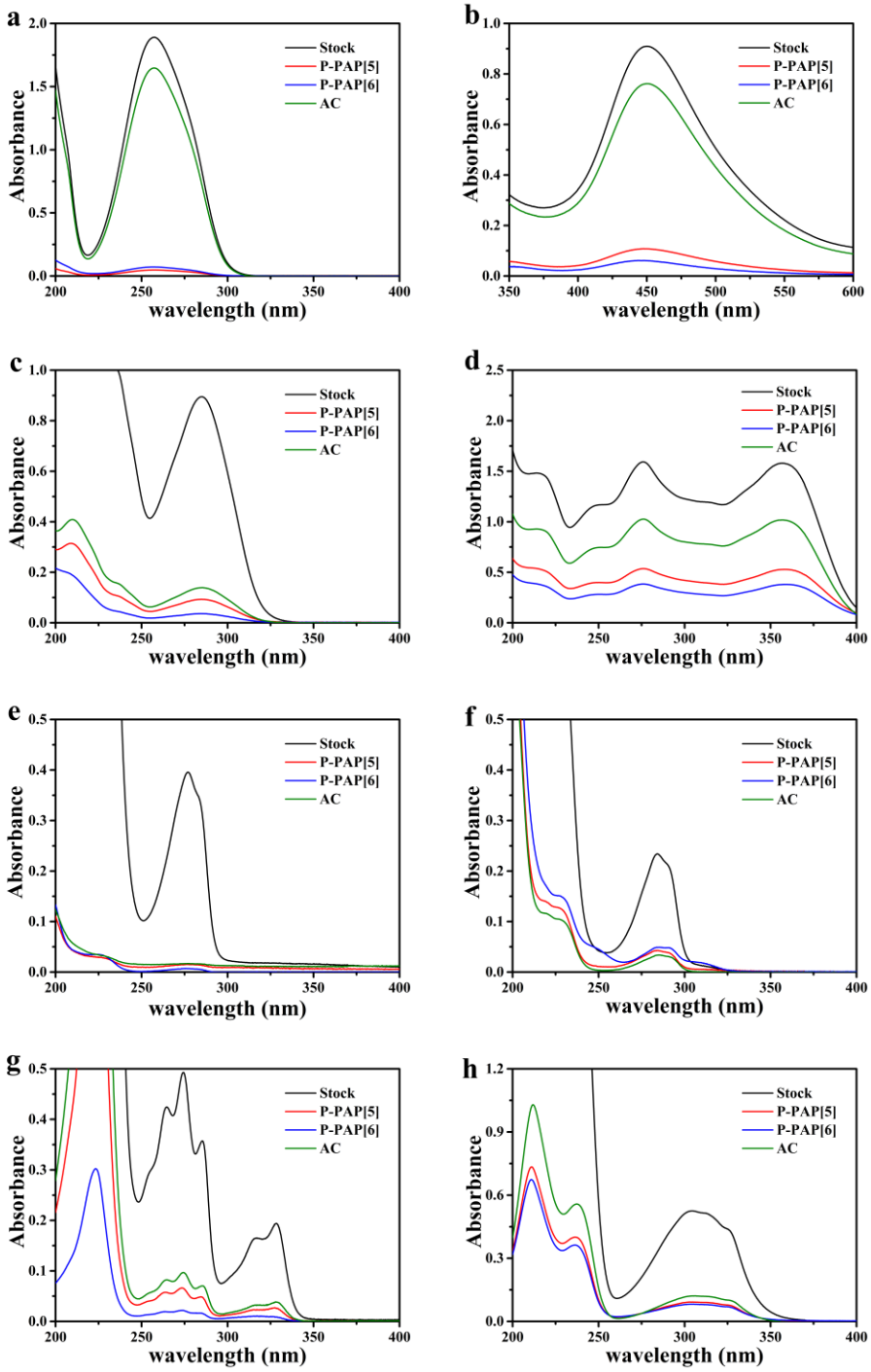

Fig. S6 UV-Vis spectra of (a) paraquat (λ = 257 nm), (b) Cu^{2+} (λ = 450 nm), (c) carbamazepine (λ = 285 nm), (d) tetracycline (λ = 276 nm), (e) BPA (λ = 277 nm), (f) 2,4-DCP (λ = 284 nm), (g) 2-NO (λ = 274 nm) and (h) 1-NA (λ = 305 nm) before and after adsorption with P-PAP[5], P-PAP[6] or activated carbon (AC) to determine the pollutant removal efficiency in flow-through adsorption experiments.

Paraquat adsorption kinetics of P-PAP[5] and AC

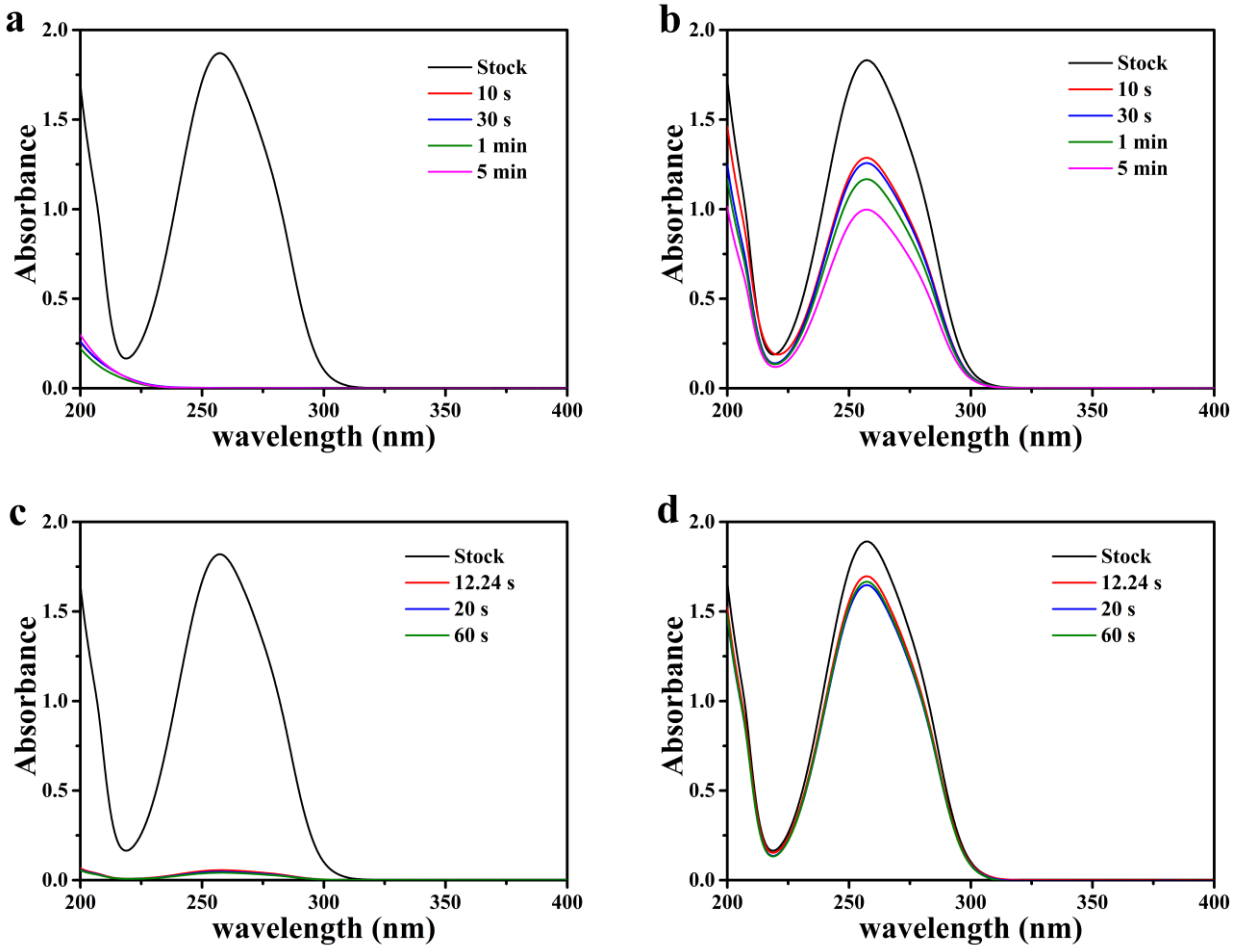

Fig. S7 UV-Vis spectra of paraquat removal assays for (a) P-PAP[5], batch adsorption; (b) AC, batch adsorption; (c) P-PAP[5], flow-through adsorption; (d) AC, flow-through adsorption.

Regeneration experiments

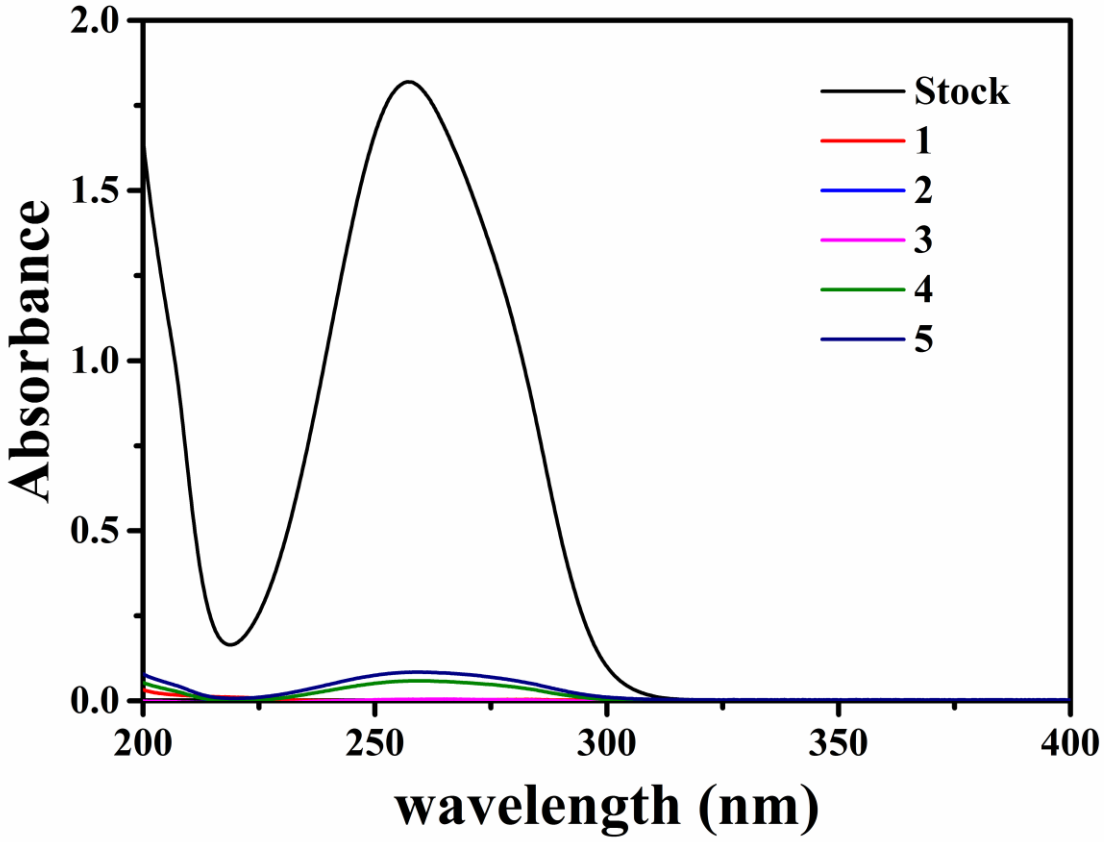

Fig. S8 UV-Vis spectra of paraquat solution after adsorption with regenerated P-PAP[5].

^{1}H NMR demonstration of host-guest interaction

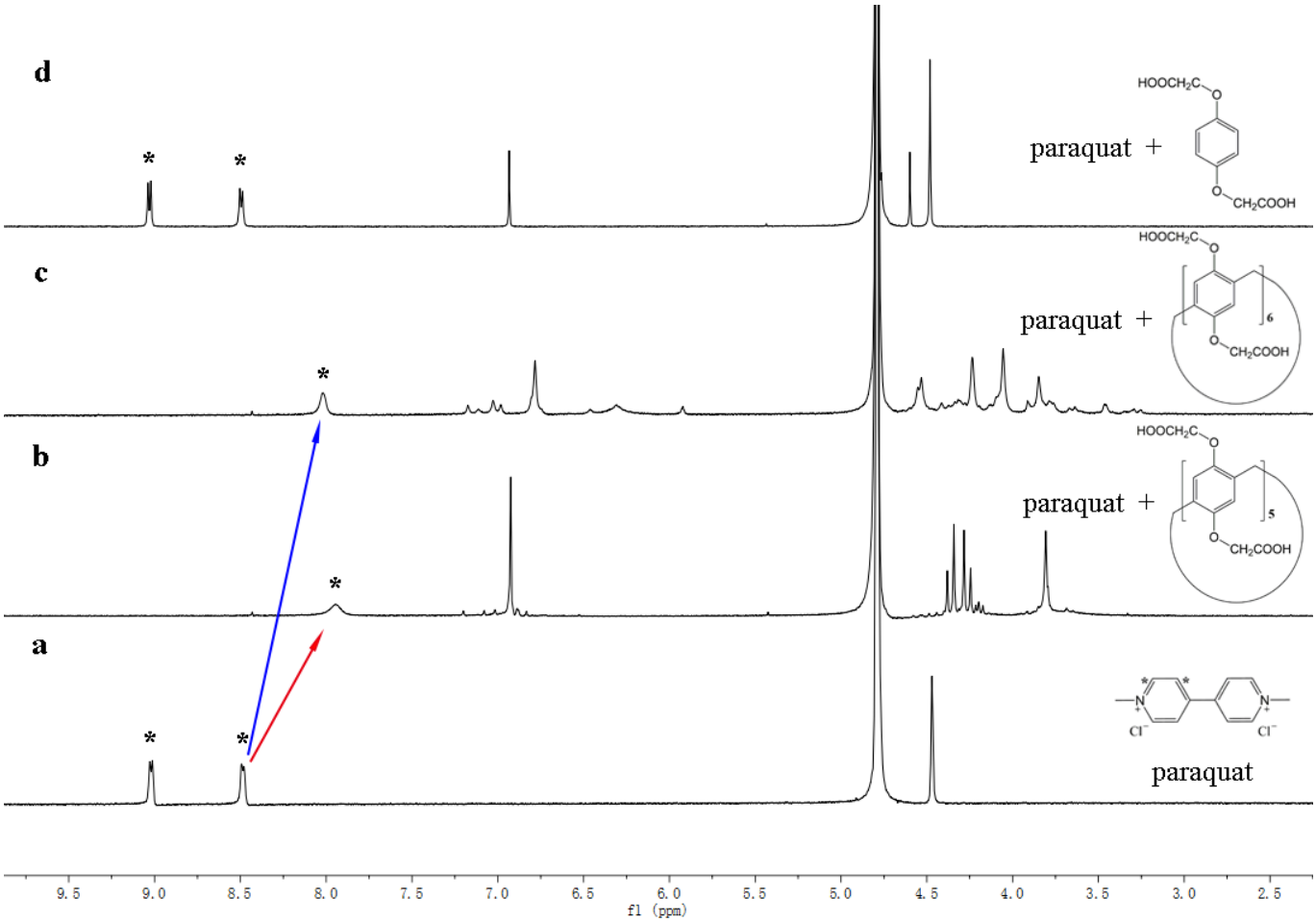

Fig. S9 ^{1}H NMR spectra recorded for (a) paraquat, (b) paraquat (1 mM) and water soluble PA[5] (1 mM), (c) paraquat (1 mM) and water soluble PA[6] (1mM), and (d) paraquat (1 mM) and monomer (6 mM) in D_2O. Asterisks indicate the aromatic protons of paraquat. Arrows show the upfield shift of paraquat aromatic protons, when water soluble PA[n]s are present.

Paraquat removal performance of various adsorbents

Type	Adsorbent	q_{max} (mg g^{-1})	k_2 (g mg^{-1} min^{-1})
Polymer	**P-PAP[5]**	**209**	**33.3**
Clay and mineral	Algerian bentonite[4]	111	—
	Soil organic matter[5]	51	—
	HA–goethite[6]	11	—
	Montmorillonite[7]	134	—
	Iron oxide–quartz[8]	0.7	—
	Treated diatomaceous earth[9]	18	0.036-0.108
	Activated bleaching earth[10]	40	0.022-0.33
	Activated clay[11]	58	0.009-0.098
	Regenerated spent bleaching earth[12]	25	0.009-0.29
	DHAPS-Montmorillonite[13]	89	0.09-0.22
	Organoclays[14]	57	—
	Acid tropical soils[15]	7	—
zeolite	Phillipsite–faujasite tuff[16]	7	—
	Modified zeolite Y[17]	69	—
	MCM-41 [18]	107	0.32-1.13
	Amino acid-modified mesoporous silicas[19]	115	0.0024-0.022
	Pillar[5,6]arene-functionalized silicas[20]	64	—
carbon	Activated carbon[21]	76	0.08-6.45
	3D graphene[22]	119	0.00062-0.00073
	Activated carbon[23]	160	0.35-0.66
Acid	Humic acid[24]	216	—
	Fulvic acid[24]	100	—
Gel	Polyacrimide/ methylcellulose hydrogels[25]	14	—

Biomass	Methacrylic acid modified rice husk[26,27]	293, 318	—
	Swine-manure-derived biochar[28]	—	0.0031-0.015
	Ayous sawdust[29]	9	6.08
	TEMPO-oxidized pulp[30]	174	0.017-0.079
Polymer	Carbon-coated electrospun fiber[31]	438	0.0008-0.0019

Table S1 Maximum adsorption capacity (q_{max}) and pseudo-second-order kinetic model constant (k_2) of various adsorbents for paraquat removal. Different conditions are applied to measure the adsorption capacity and kinetics.

References

1 T. Ogoshi, S. Kanai, S. Fujinami, T. A. Yamagishi and Y. Nakamoto, *J. Am. Chem. Soc.*, 2008, **130**, 5022–5023.

2 X. B. Hu, Z. X. Chen, L. Chen, L. Zhang, J. L. Hou and Z. T. Li, *Chem. Commun.*, 2012, **48**, 10999–11001.

3 M. Kompany-Zareh, a. Massoumi and H. Tavallali, *Microchem. J.*, 1999, **63**, 257–265.

4 D. Ait Sidhoum, M. M. Socías-Viciana, M. D. Ureña-Amate, A. Derdour, E. González-Pradas and N. Debbagh-Boutarbouch, *Appl. Clay Sci.*, 2013, **83**–**84**, 441–448.

5 D. Gondar, R. López, J. Antelo, S. Fiol and F. Arce, *J. Hazard. Mater.*, 2012, **235**–**236**, 218–223.

6 M. Brigante, G. Zanini and M. Avena, *J. Hazard. Mater.*, 2010, **184**, 241–247.

7 R. Guégan, M. Giovanela, F. Warmont and M. Motelica-Heino, *J. Colloid Interface Sci.*, 2015, **437**, 71–79.

8 M. Pateiro-Moure, A. Bermúdez-Couso, D. Fernández-Calviño, M. Arias-Estévez, R. Rial-Otero and J. Simal-Gándara, *J. Chem. Eng. Data*, 2010, **55**, 2668–2672.

9 W. T. Tsai, K. J. Hsien, Y. M. Chang and C. C. Lo, *Bioresour. Technol.*, 2005, **96**, 657–663.

10 W. T. Tsai, C. W. Lai and K. J. Hsien, *Chemosphere*, 2004, **55**, 829–837.

11 W. T. Tsai, C. W. Lai and K. J. Hsien, *J. Colloid Interface Sci.*, 2003, **263**, 29–34.

12 W. T. Tsai and C. W. Lai, *J. Hazard. Mater.*, 2006, **134**, 144–148.

13 Z. Gu, M. Gao, L. Lu, Y. Liu and S. Yang, *Ind. Eng. Chem. Res.*, 2015, **54**, 4947–4955.

14 Y. Seki and K. Yurdakoç, *J. Colloid Interface Sci.*, 2005, **287**, 1–5.

15 A. S. R. Juo and O. O. Oginni, *J. Environ. Qual.*, 1978, **7**, 9–12.

16 K. M. Ibrahim and H. A. Jbara, *J. Hazard. Mater.*, 2009, **163**, 82–86.

17 H. Zhang, Y. Kim and P. K. Dutta, *Microporous Mesoporous Mater.*, 2006, **88**, 312–318.

18 M. Brigante and M. Avena, *Microporous Mesoporous Mater.*, 2014, **191**, 1–9.

19 F. K. Shieh, C. T. Hsiao, J. W. Wu, Y. C. Sue, Y. L. Bao, Y. H. Liu, L. Wan, M. H. Hsu, J. R. Deka and H. M. Kao, *J. Hazard. Mater.*, 2013, **260**, 1083–1091.

20 T. Zhou, N. Song, H. Yu and Y. W. Yang, *Langmuir*, 2015, **31**, 1454–1461.

21 N. K. Hamadi, S. Swaminathan and X. D. Chen, *J. Hazard. Mater.*, 2004, **112**, 133–141.

22 Y. Huang, C. Li and Z. Lin, *ACS Appl. Mater. Interfaces*, 2014, **6**, 19766–19773.

23 J. M. Sieliechi and P. S. Thue, *Desalin. Water Treat.*, 2015, **55**, 986–998.
24 A. Iglesias, R. López, D. Gondar, J. Antelo, S. Fiol and F. Arce, *Chemosphere*, 2009, **76**, 107–113.
25 C. Guo, L. Zhou and J. Lv, *Polym. Polym. Compos.*, 2013, **21**, 449–456.
26 S. T. Hsu, L. C. Chen, C. C. Lee, T. C. Pan, B. X. You and Q. F. Yan, *J. Hazard. Mater.*, 2009, **171**, 465–470.
27 S. T. Hsu and T. C. Pan, *Bioresour. Technol.*, 2007, **98**, 3617–3621.
28 W. T. Tsai and H. R. Chen, *Int. J. Environ. Sci. Technol.*, 2013, **10**, 1349–1356.
29 C. P. Nanseu-Njiki, G. K. Dedzo and E. Ngameni, *J. Hazard. Mater.*, 2010, **179**, 63–71.
30 K. Y. A. Lin, Y. T. Heish, T. Y. Tsai and C. F. Huang, *Cellulose*, 2015, **22**, 3261–3274.
31 R. Zhao, Y. Wang, X. Li, B. Sun, Y. Li, H. Ji, J. Qiu and C. Wang, *ACS Sustain. Chem. Eng.*, 2016, **4**, 2584–2592.